Journal of Materials Chemistry A

ROYAL SOCIETY OF CHEMISTRY

PAPER

View Article Online
View Journal | View Issue

Cite this: J. Mater. Chem. A, 2021, 9, 19788

Enhancing hydrogen production by photobiocatalysis through *Rhodopseudomonas palustris* coupled with conjugated polymers†

Zijuan Wang,[a] Dong Gao,[b] Hao Geng[a] and Chengfen Xing *[ab]

Received 3rd February 2021
Accepted 31st March 2021

DOI: 10.1039/d1ta01019k

rsc.li/materials-a

Utilizing solar energy for hydrogen production by combining light-activated materials and biocatalysts has become a promising alternative to fossil fuels. Herein, a feasible and simple bio-hybrid complex based on water-soluble oligofluorene (OF), polythiophene (PTP) and *Rhodopseudomonas palustris* (*R. palustris*), one kind of photosynthetic bacteria, was constructed for enhancing photocatalytic hydrogen production. Under the irradiation of visible light, there was fluorescence resonance energy transfer (FRET) between OF and PTP, which amplified photoelectron signals and transferred electrons *via* PTP to methyl viologen (MV^{2+}), an electron mediator that established electron transfer pathways between organic materials and *R. palustris*. Hydrogen production involving *R. palustris* was catalyzed by nitrogenase. It is noteworthy that MV^{2+} was reduced to $MV^{+\bullet}$ and transferred electrons to nitrogenase in *R. palustris*, converting protons and electrons to molecular hydrogen. Besides, triethanolamine (TEOA) was added as an electron donor to provide electrons to PTP. The proposed OF/PTP/MV^{2+}/TEOA/*R. palustris* system provided a feasible strategy for photocatalytic hydrogen production with low-cost and easily implemented techniques.

Introduction

Photocatalytic hydrogen production is cost-effective for the storage of solar energy in chemical fuels, and it is a sustainable strategy to overcome energy shortages and environmental issues.[1–3] Biohydrogen production methods are efficient hydrogen formation ways, and researchers have focused on the semi-artificial photosynthetic field coupling specific enzymes for biocatalysts and light-activated materials, such as inorganic semiconductors and molecular photosensitizers.[4,5] These hybrid systems integrate effective solar energy conversion of materials and selective catalysis of enzymes, which has been widely applied for light-driven hydrogen production.[6–8] For example, purified [FeFe]-hydrogenase or nitrogenase was modified on the surface of inorganic semiconductors (*e.g.*, cadmium sulfide (CdS) and titanium dioxide (TiO_2)) to realize photocatalytic hydrogen production.[9] However, time-consumption and cumbersome operations to obtain purified enzymes hinder their practical application.[10,11]

The application of whole-cells is an emerging method that utilizes the photocatalytic activity of semiconductor materials and the stability of enzymes in microorganisms for photocatalytic hydrogen production.[12] These biological hybrids avoid complicated genetic techniques and purification steps and are easily scaled up and widely adopted.[13,14] For photocatalytic hydrogen production, such a cell-based strategy was constructed by the combination of TiO_2, methyl viologen (MV^{2+}) as an electron mediator, and recombinant *Escherichia coli*.[15] MV^{2+} was required to collect photoelectrons and establish an electron transfer pathway in a cell-based photocatalytic hydrogen production hybrid composed of a water-soluble dye and *Shewanella oneidensis*.[16] In addition, the hydrogen production efficiency can be increased by 90 times based on enhancing the reduction of MV^{2+} with an inorganic semiconductor in a bio-hybrid.[17] Recently, a cell-based strategy has been achieved through the CdS nanoparticles coated on the surface of the photoheterotrophic bacterium, *Rhodopseudomonas palustris* (*R. palustris*), and this bio-hybrid produces hydrogen under visible light while producing other chemicals with nitrogenase.[18] The classical methods of photocatalytic hydrogen production using bio-hybrids include direct or indirect photolysis, in which electron–hole separation depends on photocatalytic materials and the fermentation process using facultative anaerobic and obligate anaerobic bacteria.[19] Photocatalytic materials are crucial factors in photocatalytic hydrogen production which determine the light absorption and the production of photoelectrons.[20–22]

Conjugated polymers (CPs) are polymers with a large delocalized π-conjugated backbone in the main chain, and show semiconductor properties and can be used as photosensitizers for light-induced hydrogen formation.[23–25] Compared with

[a]School of Materials Science and Engineering, Hebei University of Technology, Tianjin 300130, P. R. China. E-mail: xingc@hebut.edu.cn

[b]Key Laboratory of Hebei Province for Molecular Biophysics, Institute of Biophysics, Hebei University of Technology, Tianjin 300130, P. R. China

† Electronic supplementary information (ESI) available. See DOI: 10.1039/d1ta01019k

photosensitive dyes and inorganic semiconductors, CPs have many excellent characteristics, such as good photoelectric properties in electrochemical devices, light harvesting, light stability for CO_2 reduction, tunable energy levels in photovoltaic cells, and biocompatibility with organisms in biological applications.[26–34] Owing to the outstanding properties of CPs, our group reported a CP-based bio-optical composite to augment photosynthesis of *R. palustris*.[35] The proposed method opens up a feasible way to use CPs for photocatalytic hydrogen production.

In this work, we constructed an efficient bio-hybrid photocatalytic hydrogen production complex, in which water-soluble oligofluorene (OF) and polythiophene (PTP) serve as superior photosensitizers combined with *R. palustris* as a biocatalyst. Under the irradiation of visible light, there is fluorescence resonance energy transfer (FRET) between OF and PTP, which can amplify photoelectron signals and transfer electrons to microorganisms for hydrogen production. Moreover, MV^{2+} was added as an electron mediator in the complex to permeate cells and facilitate electron transfer between the OF/PTP pair and nitrogenase in *R. palustris*, and triethanolamine (TEOA) was used as a sacrificial electron donor. In the OF/PTP/MV^{2+}/TEOA/*R. palustris* bioorganic complex, separated electrons of the OF/PTP pair continuously provided by TEOA were delivered to MV^{2+}, and then MV^{2+} was reduced to blue $MV^{+\bullet}$ under illumination. After that, $MV^{+\bullet}$ transferred the electrons *via* the nitrogenase in intact *R. palustris*, making it accept more electrons to enhance hydrogen synthesis. This bio-hybrid system provided a fossil-fuel-free, efficient and clean way for hydrogen production through natural enzymes and organic photosensitizers (Scheme 1).

Results and discussion

The preparation methods of PTP and OF have been reported in previous literature.[36,37] Their excellent optical properties were attributed to thiophene units on PTP and fluorene units on OF, and their water solubility arose from carboxyl and guanidine groups in the side chains respectively. The absorption peak of OF in the visible light region was observed at 370 nm and that of PTP was observed at 410 nm. The emission peaks of OF were observed at 440 and 470 nm, and that of PTP was observed at 550 nm (Fig. 1a). There was a good overlap between the fluorescence emission spectrum of OF and the absorption spectrum of PTP, which satisfied the energy transfer conditions through the FRET mechanism.[38,39] As shown in Fig. 1b, the fluorescence intensity of OF decreased gradually as the concentration of PTP increased, which indicated the energy transfer from OF to PTP. The ratio of the emission intensity at 440 nm and 550 nm ($I_{440\ nm}/I_{550\ nm}$) gradually increased and the fluorescence intensity of OF decreased by 12.8 times which was also verified by the trend of FRET from OF to PTP (ESI Fig. S1†). MV^{2+} as an electron mediator that was often used in artificial hydrogen producing systems was added in the complex to transfer electrons.[40–42] Fig. 1c shows that the fluorescence intensity of PTP was gradually quenched with the addition of MV^{2+} , indicating electron

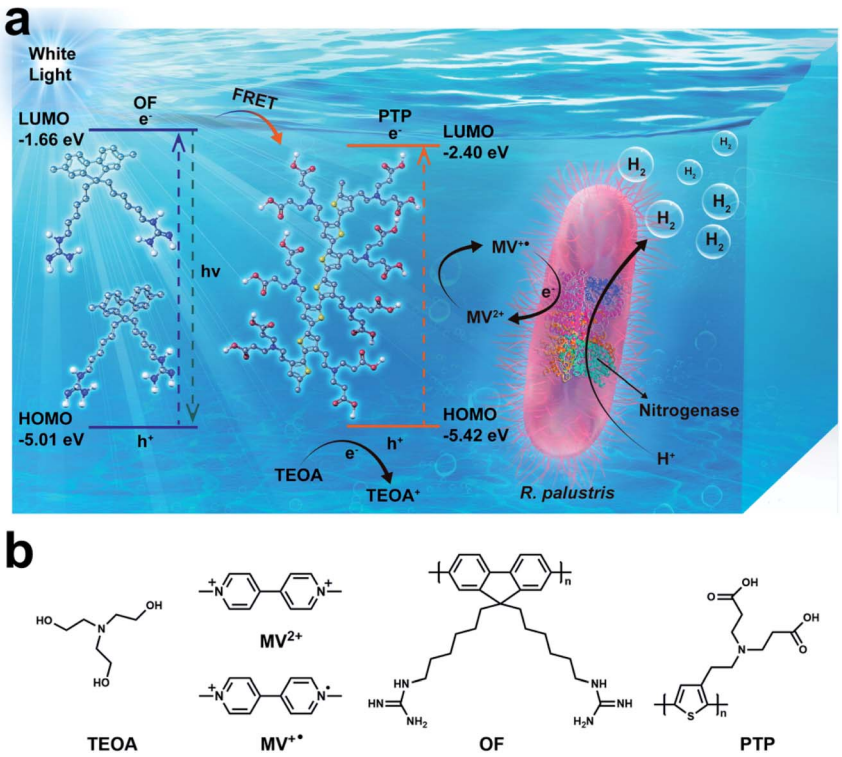

Scheme 1 (a) Bio-hybrid photocatalytic hydrogen production complex. There are four parts in this system: OF and PTP as photosensitizers, MV^{2+} as an electron mediator, TEOA as an electron donor and *R. palustris* as a biocatalyst. (b) Chemical structures of TEOA, MV^{2+}, $MV^{+\bullet}$, OF and PTP.

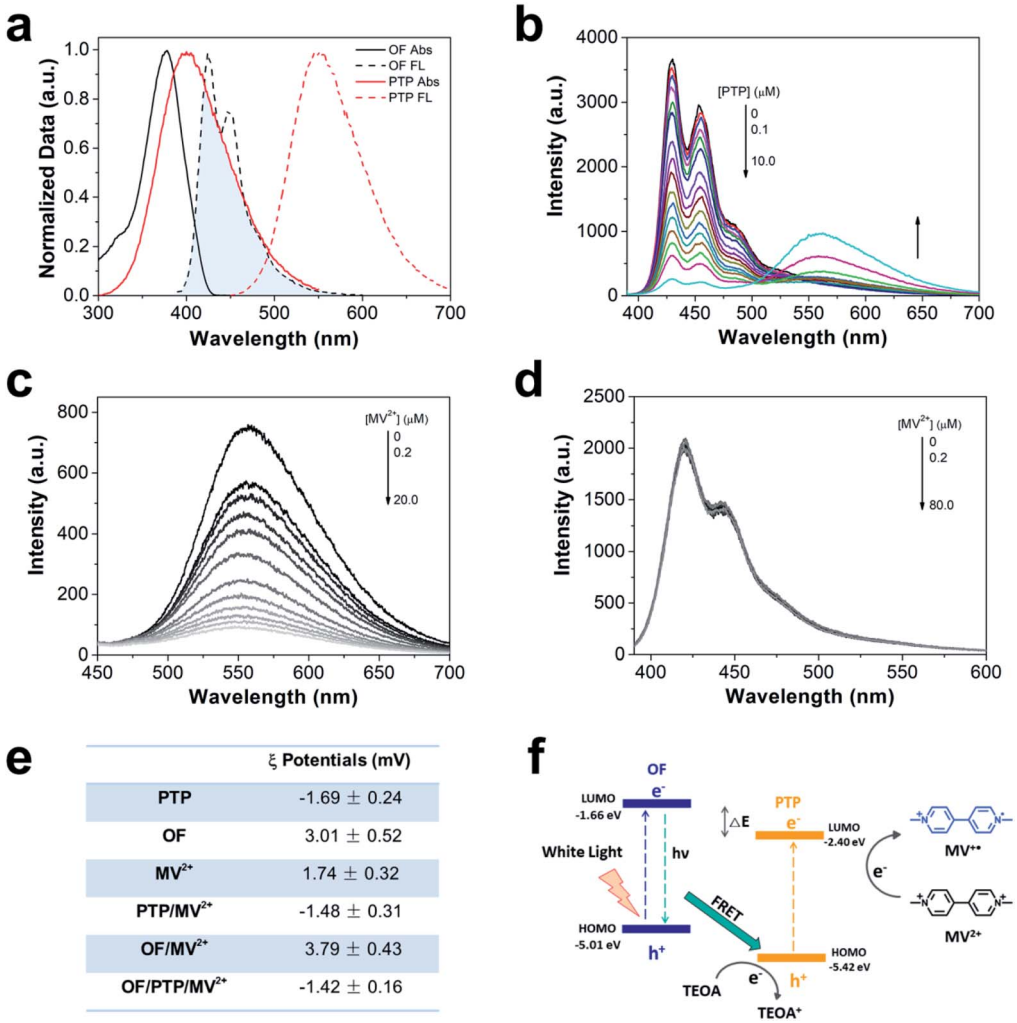

e

	ξ Potentials (mV)
PTP	-1.69 ± 0.24
OF	3.01 ± 0.52
MV^{2+}	1.74 ± 0.32
PTP/MV^{2+}	-1.48 ± 0.31
OF/MV^{2+}	3.79 ± 0.43
OF/PTP/MV^{2+}	-1.42 ± 0.16

Fig. 1 The characteristics of the OF/PTP/MV^{2+}/TEOA complex. (a) Normalized UV-vis absorption spectra and fluorescence spectra of OF and PTP. (b) Fluorescence intensity of OF with increasing concentration of PTP. [OF] = 1 μM, [PTP] = 0–10.0 μM. (c) Fluorescence intensity of PTP with successive addition of MV^{2+}. [PTP] = 10 μM, [MV^{2+}] = 0–20 μM. (d) Fluorescence intensity of OF with successive addition of MV^{2+}. [OF] = 1 μM, [MV^{2+}] = 0–80 μM. (e) ζ potentials of PTP, OF, MV^{2+}, PTP/MV^{2+}, OF/MV^{2+} and OF/PTP/MV^{2+}. [PTP] = 20 μM, [OF] = 20 μM, [MV^{2+}] = 500 μM. (f) Schematic diagram of the electron transfer pathway of the OF/PTP/MV^{2+}/TEOA complex under illumination.

transfer from PTP to MV^{2+}. The Stern–Volmer constant (K_{sv}) was calculated by measuring the fluorescence of PTP *via* the Stern–Volmer equation (eqn (1)).

$$I_0/I = 1 + K_{sv}[Q] \quad (1)$$

Under low concentrations of MV^{2+} (0–1.0 μM), the K_{sv} value was 1.78×10^6 M^{-1} from the linear Stern–Volmer plot, indicating the quenching of the fluorescence intensity of PTP by MV^{2+} (ESI, Fig. S2†). However, there was no explicit interaction between MV^{2+} and OF with the increase of MV^{2+} concentration (Fig. 1d). Both OF and MV^{2+} have positive charge properties, leading to electrostatic repulsive interactions, which made it difficult for MV^{2+} to obtain electrons from OF. In contrast, negative charge properties of PTP made the electrons transfer from PTP to MV^{2+} more easily than from OF (Fig. 1e). As shown in ESI Fig. S3,† in the case of electron donor TEOA and CPs, the fluorescence of OF remained at the same level, while the fluorescence of PTP increased with the concentration of TEOA. In addition, the OF/PTP/MV^{2+}/TEOA complex formed aggregates with a hydrodynamic diameter of about 700 nm, which was consistent with the OF/PTP/TEOA complex through dynamic light scattering (DLS) measured, indicating that MV^{2+} had no effect on its assembly in solution (ESI, Fig. S4†). The schematic diagram of energy transfer among the OF/PTP pair, TEOA and MV^{2+} is shown in Fig. 1f. Electron–hole separation occurred when OF and PTP acted as photosensitizers under light illumination. The HOMO and LOMO energy level offset between OF and PTP both exceeded 0.3 eV (ESI, Fig. S5†), which provided a sufficient driving force for the hole/electron dissociation of the OF/PTP pair.[43] Due to the energy which is able to transfer from OF to PTP through FRET and the electrostatic interaction between PTP and MV^{2+}, MV^{2+} was reduced to $MV^{+\bullet}$ (blue) by separated electrons from the OF/PTP pair, and the electrons

missing from the holes were supplied by TEOA. The OF/PTP/MV^{2+}/TEOA complex established an efficient electron transfer pathway through FRET between OF and PTP to MV^{2+}.

To deeply investigate the generation of electrons in the OF/PTP/MV^{2+}/TEOA complex, the absorption of $MV^{+\bullet}$ at 605 nm was determined under illumination for one hour. Compared with other complexes, the OF/PTP/MV^{2+}/TEOA complex produced the most $MV^{+\bullet}$ as shown in Fig. 2a. However, there were few $MV^{+\bullet}$ ions produced by MV^{2+}/TEOA and OF/PTP/MV^{2+}/TEOA complexes. Owing to the transfer of electrons to MV^{2+} through the FRET between OF and PTP in the OF/PTP/MV^{2+}/TEOA complex, the production of $MV^{+\bullet}$ was greatly increased. To study the process of $MV^{+\bullet}$ production in the OF/PTP/MV^{2+}/TEOA complex, the UV-visible spectrum of the complex was measured under illumination for 20 min (Fig. 2b). Upon extension of the illumination time, the absorption of reduced $MV^{+\bullet}$ at both 395 and 603 nm gradually increased and the solution changed from yellow to blue as a result of gradual accumulation of $MV^{+\bullet}$. These results indicated that the OF/PTP pair satisfied the requirements of photosensitizers and could effectively reduce MV^{2+} to $MV^{+\bullet}$.

It was documented that MV^{2+} acted as an electron mediator that permeated bacterial cells and established a pathway to transfer electrons from chemical reductants to microbial enzymes.[44] Sodium dithionite, a chemical reductant that can easily reduce MV^{2+} to $MV^{+\bullet}$, was used to evaluate whether $MV^{+\bullet}$ could reduce enzymes of *R. palustris* to produce hydrogen. Sodium dithionite was added to a sealed 3 mL sample containing MV^{2+} and *R. palustris* filled with argon for 30 min to determine its hydrogen production. As the largest amount of hydrogen production strategy, the complex of sodium dithionite, MV^{2+} and *R. palustris* produced 624.80 nmol hydrogen in 30 min as shown in Fig. 3a. The proposed complex produced 247.01 nmol hydrogen in the absence of MV^{2+}, while it could not generate hydrogen without *R. palustris*. These results implied that MV^{2+} was an effective promoter that transferred the acquired electrons to *R. palustris* and effectively increased the production of hydrogen. Here, *R. palustris* as a natural catalyst combined with OF and PTP as photosensitizers was used in the OF/PTP/MV^{2+}/TEOA/*R. palustris* complex for photocatalytic hydrogen production. The proposed OF/PTP/MV^{2+}/TEOA/*R. palustris* complex was able to produce the largest amount of hydrogen with irradiation for 2 h, while no hydrogen was generated in the absence of *R. palustris* as shown in Fig. 3b. In addition, illumination played a crucial role in the photocatalytic hydrogen production process using the OF/PTP/MV^{2+}/TEOA/*R. palustris* complex, in which hydrogen production fell sharply in the absence of irradiation (ESI, Fig. S6†). Compared with other systems for hydrogen production with and without photosynthetic organisms (ESI, Table S1†), the OF/PTP/MV^{2+}/TEOA/*R. palustris* complex exhibited some excellent characteristics, such as efficient hydrogen production, low-cost and simple operation. The results suggested the feasibility of the enzyme catalyzed for hydrogen production using the OF/PTP/MV^{2+}/TEOA/*R. palustris* complex.

Hydrogen production using the OF/PTP/MV^{2+}/TEOA/*R. palustris* complex at different pHs and light intensities was deeply investigated. The influence of pH on hydrogen production using the OF/PTP/MV^{2+}/TEOA/*R. palustris* complex is shown in Fig. 4a. It produced the largest amount of hydrogen at a pH of 7 under biocatalyst-friendly conditions. The hydrogen production decreased gradually as the pH value changed from 6 to 5 with the acidification of the solution. The changes in pH affected the transfer of electrons from $MV^{+\bullet}$ to the enzyme and inhibited the biological enzyme activity of *R. palustris*. Under the conditions of pH 8 and pH 9, the decrease in hydrogen production was mainly due to the influence of the proton gradient on the *R. palustris* cell, which affects ATP synthesis of photophosphorylation. With the increase of light intensity, the hydrogen production of the bio-hybrid system gradually increased (Fig. 4b). When it reached 8 mW cm^{-2}, the hydrogen production was the most. When the light intensity was further enhanced, the hydrogen production decreased gradually. The catalytic activity of *R. palustris* was destroyed by high light intensity. The hydrogen production process of electron transfer to *R. palustris* in the OF/PTP/MV^{2+}/TEOA/*R. palustris* complex was subject to the regulation of enzyme activity by stimulus conditions.

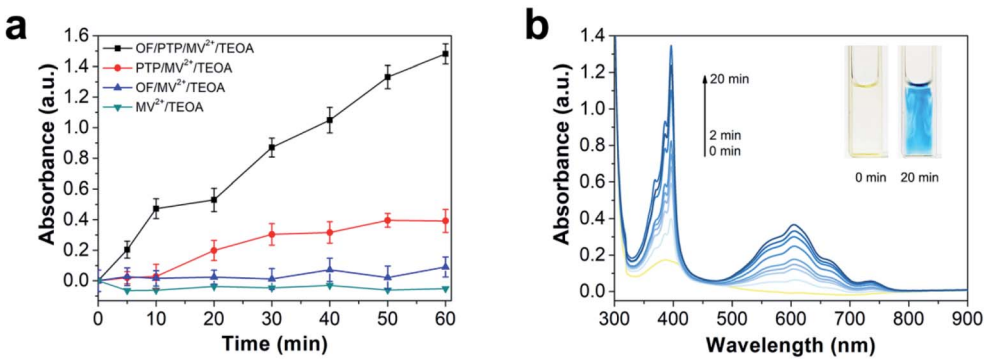

Fig. 2 The production of $MV^{+\bullet}$ in the OF/PTP/MV^{2+}/TEOA complex under illumination conditions. (a) The absorption of $MV^{+\bullet}$ at 605 nm in OF/PTP/MV^{2+}/TEOA, PTP/MV^{2+}/TEOA, OF/MV^{2+}/TEOA and TEOA/MV^{2+} complexes under irradiation at 10 mW cm^{-2} for 1 h. (b) UV-visible spectra of the OF/PTP/MV^{2+}/TEOA complex under irradiation at 10 mW cm^{-2} for 20 min; the light yellow line at 0 min, the dark blue line at 20 min; inset: photographs of the solution before and after irradiation for 20 minutes. [OF] = 20 μM, [PTP] = 20 μM, [MV^{2+}] = 5 mM, 1% TEOA (v/v). The error bars show the standard deviation of three independent experiments.

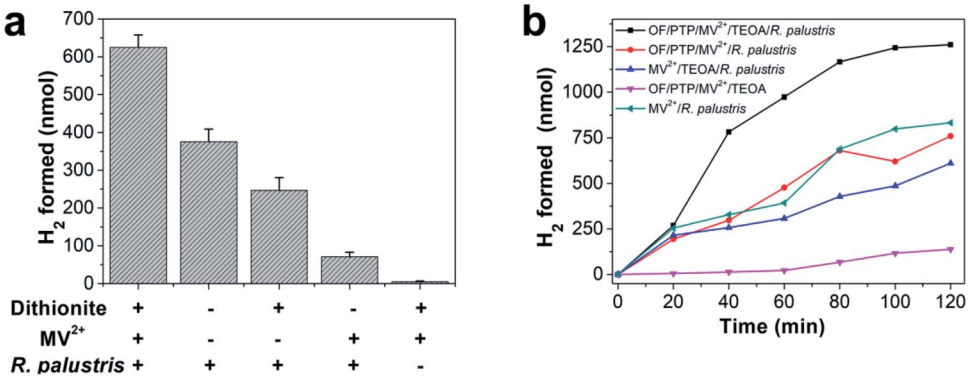

Fig. 3 Hydrogen production of the OF/PTP/MV^{2+}/TEOA/*R. palustris* complex. (a) Hydrogen production of dithionite, MV^{2+} and *R. palustris* in different complexes under anaerobic conditions for 30 min ("−" indicates that the complex had not been treated accordingly, and "+" indicates that the system had been treated under these conditions). (b) H_2 production of different complexes under irradiation at 10 mW cm^{-2} for 120 min. Light intensity was 10 mW cm^{-2}, [OF] = 20 μM, [PTP] = 20 μM, [MV^{2+}] = 500 μM, 1% TEOA (v/v). The optical density at 660 nm in 10 mM phosphate-buffered saline (PBS) solution was 1.

The capability of the OF/PTP/MV^{2+}/TEOA/*R. palustris* complex for photocatalytic hydrogen production is well established. In the process of hydrogen production involving *R. palustris*, nitrogenase reduced protons into molecular hydrogen and fixed molecular nitrogen.[45,46] Fig. 5a shows the diagram of hydrogen production by using the OF/PTP/MV^{2+}/TEOA/*R. palustris* complex. $MV^{+\bullet}$ transferred electrons to nitrogenase, and was oxidized to MV^{2+}. Then the electrons and protons generated hydrogen under the catalysis of nitrogenase. In order to verify the mechanism of photocatalytic hydrogen production using the OF/PTP/MV^{2+}/TEOA/*R. palustris* complex, the protein containing nitrogenase was extracted for subsequent experiments. The whole protein electrophoresis diagram of *R. palustris* is shown in ESI Fig. S7,† which illustrated the existence of nitrogenase in *R. palustris*. The different conditions of hydrogen production with nitrogenase, the OF/PTP/MV^{2+}/TEOA complex and illumination were deeply investigated in Fig. 5b. Maximum hydrogen production was obtained by using the OF/PTP/MV^{2+}/TEOA complex, reaching 48.49 nmol. In the absence of the OF/PTP/MV^{2+}/TEOA complex or nitrogenase, hydrogen production was about 40% of that obtained by using the OF/PTP/MV^{2+}/TEOA complex. Without illumination and in the absence of nitrogenase, the proposed OF/PTP/MV^{2+}/TEOA complex could not produce any hydrogen. The results showed the feasibility of the light induction complex of OF/PTP/MV^{2+}/TEOA to catalyze hydrogen production by using biological enzymes.

Experimental methods

Materials

Two typical conjugated polymers PTP and OF were synthesized according to previous literature.[47,48] *R. palustris* (AS1.2352) was purchased from Beijing BeNa Culture Co., Ltd. (China). All other chemicals were purchased from Aladdin, Sigma and used as received.

Instruments

UV-vis absorption spectra were measured on a SPECORD 250 PLUS (Germany). Fluorescence spectra were measured on a Hitachi F-4600 fluorescence spectrophotometer (Japan). Dynamic light scattering (DLS) and ζ potentials were measured using a Malvern Nano-ZS90 (UK). The irradiation source of visible light was a MEJIRO GENOSSEN MVL-210 (Japan).

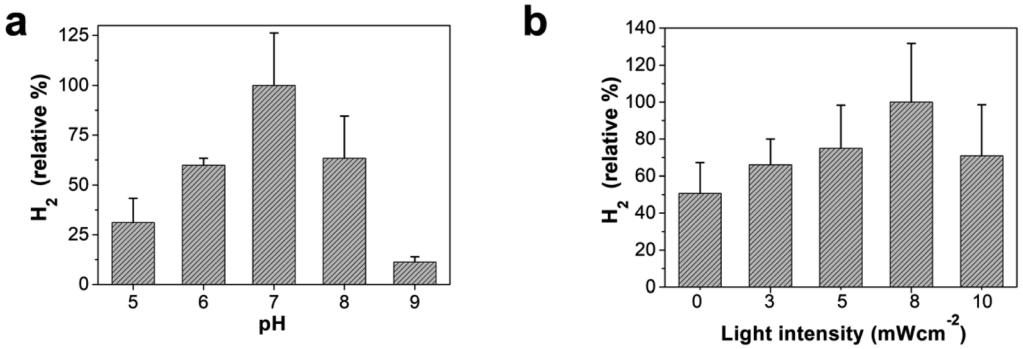

Fig. 4 The effect of pH and light intensity on H_2 production using the OF/PTP/MV^{2+}/TEOA/*R. palustris* complex. (a) H_2 production using the OF/PTP/MV^{2+}/TEOA/*R. palustris* complex at different pH. (b) H_2 production using the OF/PTP/MV^{2+}/TEOA/*R. palustris* complex at different light intensities. [OF] = 20 μM, [PTP] = 20 μM, [MV^{2+}] = 500 μM, 1% TEOA (v/v). The optical density at 660 nm in 10 mM PBS solution was 1.

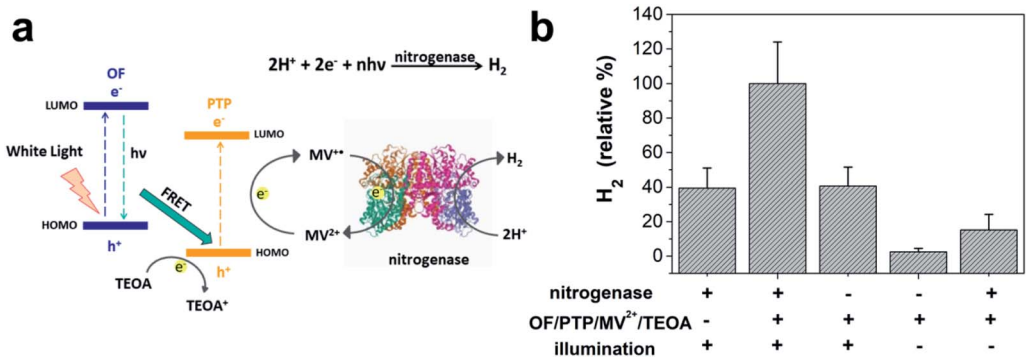

Fig. 5 Hydrogen production with nitrogenase extracted from *R. palustris*. (a) Schematic diagram of H_2 production using the OF/PTP/MV^{2+}/TEOA/*R. palustris* complex. (b) Hydrogen production with nitrogenase, the OF/PTP/MV^{2+}/TEOA complex and illumination under anaerobic conditions for 30 min ("−" indicates that the complex has not been treated accordingly, and "+" indicates that the complex has been treated under these conditions). The concentration of the crude protein of nitrogenase used in the experiment was 100 μg, light intensity was 10 mW cm^{-2}, [OF] = 20 μM, [PTP] = 20 μM, [MV^{2+}] = 500 μM, 1% TEOA (v/v).

Electrochemical measurements were performed on a CH Instruments CHI600E (China). The analysis of hydrogen production was performed on a CEAULIGHT GC-7900 gas chromatograph with argon as the carrier gas. The pH was measured using a Sartorius PB-10 (Germany).

Concentration of CPs

$$[\mathrm{CPs}] = m_{\mathrm{cp}}/(M_{\mathrm{cp}} \times V_{\mathrm{solution}})$$

[CPs] is the concentration of CPs, m_{cp} is the mass of CPs, M_{cp} is the molar mass of the repeating unit in CPs, and V_{solution} is the volume of the solution.

Detection of ζ potential

20 μM PTP, 20 μM OF and 500 μM MV^{2+} aqueous solution was prepared for ζ potential measurements. Then aqueous solutions of PTP/MV^{2+}, OF/MV^{2+} and OF/PTP/MV^{2+} complexes with the above concentrations were prepared as well. The potential was measured at 25 °C for 120 s, and the average was obtained three times to obtain the zeta potential value.

DLS measurements

The solutions of OF/PTP/TEOA and OF/PTP/MV^{2+}/TEOA complexes were prepared for size measurements. The concentrations involved in the above systems design were 20 μM PTP, 20 μM OF, 500 μM MV^{2+} and 1% (v/v) TEOA. All experiments were performed at 25 °C for 120 s, and the average was obtained three times to obtain the size value.

Fluorescence quenching experiments

The fluorescence spectrum of PTP (10 μM) solution with the increase of the concentration of MV^{2+} (0–20 μM) was measured. Then the fluorescence spectrum of OF (1 μM) solution with the increase of the concentration of MV^{2+} (0–80 μM) was measured. The excitation maxima of PTP and OF were at 390 nm and 420 nm respectively.

Detection of $MV^{+\bullet}$ accumulation

A mixed solution containing PTP (20 μM), OF (20 μM), TEOA (v/v = 1%) and MV^{2+} (5 mM) was placed in a special quartz cell and covered with a sealing rubber stopper. The solution was bubbled with argon gas for 30 min to remove oxygen in the system under 10 mW cm^{-1} irradiation. The UV-vis absorption spectrum of the solution was measured every 10 min until the accumulated light time reached the end of 2 hours. All the experiments were repeated three times.

R. palustris culture

This strain was grown on 112 van Niel's yeast agar[49] under the conditions of 1.0 g of K_2HPO_4, 0.5 g of $MgSO_4$, 10.0 g of yeast extract, 1000 mL of distilled water, and pH 7.0–7.4. Argon gas was pumped into the medium for exhausting the air, and then the inoculated culture solution (15% (v/v)) was added to a 20 mL serum bottle. The culture solution was placed in an incubator under anaerobic illumination for 5 days at a temperature of 30 °C until the culture solution turned dark red. The optical density at 660 nm with PBS solution (10 mM) was used as the biological index in the following experiments.[50]

Hydrogen generation using dithionite

Hydrogen production using dithionite (300 mg L^{-1}), MV^{2+} (500 μM) and *R. palustris* in different complexes was measured under anaerobic conditions for 30 min. Then the hydrogen production was determined by gas chromatography through 200 μL of the upper gas. The amount of hydrogen produced was calculated using H_2 normalized curves. All the experiments were repeated three times.

Hydrogen generation measurement using different complexes

The solutions of MV^{2+}/*R. palustris*, MV^{2+}/TEOA/*R. palustris* and OF/PTP/TEOA, OF/PTP/MV^{2+}/TEOA/*R. palustris* complexes were sealed in Pyrex bottles, bubbled with argon gas for 30 minutes and irradiated with 10 mW cm^{-1} for 2 h. Every 20 min 200 μL of the upper gas of the reactor was injected into a gas

chromatograph to measure hydrogen production for 2 h. Moreover, the hydrogen production of the OF/PTP/MV^{2+}/TEOA/*R. palustris* solution without illumination was also studied. The amount of hydrogen produced was calculated using H_2 normalized curves. All the experiments were repeated three times.

Hydrogen generation using a bio-hybrid complex at different pHs

The pH of the bio-hybrid complex was adjusted with NaOH and HCl. Mixed solutions consisting of 20 μM PTP, 20 μM OF, 500 μM MV^{2+}, 1% (v/v) TEOA and a suspension of *R. palustris* (OD_{660} = 1.0) were sealed in Pyrex bottles and bubbled with argon gas for 30 min. The mixed solutions of different pH (5, 6, 7, 8 and 9) were irradiated with 10 mW cm^{-1} for 1 h. 200 μL of the upper gas of the reactor was injected into a gas chromatograph to measure hydrogen production. The amount of hydrogen produced was calculated by using H_2 normalized curves. All the experiments were repeated three times.

Hydrogen generation using a bio-hybrid complex at different light intensities

Mixed solutions consisting of 20 μM PTP, 20 μM OF, 500 μM MV^{2+}, 1% (v/v) TEOA and a suspension of *R. palustris* (OD_{660} = 1.0) were sealed in Pyrex bottles and bubbled with argon gas for 30 min. The mixed solutions were irradiated for 1 h with different light intensities (0, 3, 5, 8, 10 mW cm^{-2}) . 200 μL of the upper gas of the reactor was injected into the gas chromatograph to measure hydrogen production. The amount of hydrogen produced was calculated by using H_2 normalized curves. All the experiments were repeated three times.

H_2 normalized curve

Standard H_2, 4.9% (v/v) H_2 in argon, was chosen as a balance gas. Two needles of different lengths were inserted into a 200 mL glass bottle with a stopper. The long needle was connected to the gas cylinder and acted as an air inlet, and the small needle was inserted into the rubber stopper to provide an air outlet. Gas exchange was performed in the glass bottle for 30 min. 20, 40, 60, 80, 100 and 120 μL of gas were injected into the GC respectively, and each one for three times. The relationship between the H_2 peak area and the number of moles of hydrogen follows the equation $y = 3.23 \times 10^6x^2 + 97\,796x$ by fitting.

Cyclic voltammetry measurements

Cyclic voltammetry (CV) measurements were carried out using a three-electrode system with a glassy carbon electrode as the working electrode, platinum wire as the counter electrode, and a Ag/AgCl electrode as the reference electrode. 2 mg PTP or OF was added into 2 mL 0.1 M tetrabutylammonium hexafluorophosphate in anaerobic acetonitrile solution to obtain electrochemical properties and the energy levels of PTP and OF were calculated at a scan rate of 0.05 V s^{-1}. $E_g = (1240/\lambda_{onset})$ eV, $E_{HOMO} = -(E_{ox} + 4.40)$ eV, $E_{LOMO} = E_{HOMO} + E_g$.

Protein extraction

To prepare the protein of *R. palustris*, the culture was harvested under anaerobic conditions by centrifugation at 8000 rpm for 5 min, and then it was washed with 1× PBS 3 times. The suspension was treated by the ultrasonic disruption method to obtain the protein of *R. palustris*. The precipitate was discarded after centrifugation at 3000 rpm for 30 min, and the supernatant contained nitrogenase protein. Protein concentrations were analyzed by the Biuret assay using BSA as the standard. The nitrogenase protein was assessed by SDS-PAGE analysis with Coomassie G-250.

Conclusions

We have established a feasible bio-hybrid complex for hydrogen production, which was based on four solid foundations: PTP and OF as water-soluble photosensitizers, MV^{2+} as an electron mediator, TEOA as an electron donor and *R. palustris* as a biocatalyst. Under the illumination of visible light, FRET between OF and PTP amplified the photoelectron signals and transferred electrons to MV^{2+}. MV^{2+} was added as an electron mediator in the complex to permeate cells and facilitate electron transfer between the OF/PTP pair and *R. palustris*. The hydrogen production of the bio-hybrid complex reached 0.63 μmol h^{-1}, which was 8.1 times higher than that of the OF/PTP/MV^{2+}/TEOA complex. The biocatalytic activity of *R. palustris* was the main factor in hydrogen production using the bio-hybrid complex and it was influenced by the change of pH and light intensity. Moreover, it has been confirmed that nitrogenase in *R. palustris* played a key role in hydrogen production using *R. palustris* as a biocatalyst. This approach provided a simple and efficient strategy for visible light-driven hydrogen production using bio-hybrid complexes of organic semiconductors and microorganisms.

Conflicts of interest

There are no conflicts to declare.

Acknowledgements

The authors are grateful to Prof. Shu Wang from Key Laboratory of Organic Solids, Institute of Chemistry, Chinese Academy of Sciences and Dr Huan Lu from Peking University (Beijing, China). The authors are also grateful for the financial support from the National Natural Science Foundation of China (no. 21773054, 21905072, 22077025 and 51803046) and the Natural Science Foundation of Hebei Province (no. B2020202062 and B2020202086).

Notes and references

1 S. F. Sousa, B. L. Souza, C. L. Barros and A. O. T. Patrocinio, *Int. J. Photoenergy*, 2019, **2019**, 23.

2 A. M. Abdalla, S. Hossain, O. B. Nisfindy, A. T. Azad, M. Dawood and A. K. Azad, *Energy Convers. Manage.*, 2018, **165**, 602–627.
3 G. Glenk and S. Reichelstein, *Nat. Energy*, 2019, **4**, 216–222.
4 Y. Honda, Y. Shinohara and H. Fujii, *Catal. Sci. Technol.*, 2020, **10**, 6006–6012.
5 S. H. Lee, D. S. Choi, S. K. Kuk and C. B. Park, *Angew. Chem., Int. Ed.*, 2018, **130**, 8086–8116.
6 H. Tong, S. Ouyang, Y. Bi, N. Umezawa, M. Oshikiri and J. Ye, *Adv. Mater.*, 2012, **24**, 229–251.
7 A. A. Ismail and D. W. Bahnemann, *Sol. Energy Mater. Sol. Cells*, 2014, **128**, 85–101.
8 Y. Ding, J. R. Bertram, C. Eckert, R. R. Bommareddy, R. Patel, A. Conradie, S. Bryan and P. Nagpal, *J. Am. Chem. Soc.*, 2019, **141**, 10272–10282.
9 K. A. Brown, M. B. Wilker, M. Boehm, G. Dukovic and P. W. King, *J. Am. Chem. Soc.*, 2012, **134**, 5627–5636.
10 E. A. Vasconcelos, R. C. Leitão and S. T. Santaella, *BioEnergy Res.*, 2016, **9**, 1260–1271.
11 S. W. M. Kengen, H. P. Goorissen, M. Verhaart, E. W. J. van Niel, P. A. M. Claassen and A. J. M. Stams, Biological hydrogen production by anaerobic microorganisms, *Biofuels*, ed. W. Soetaert, and E. J. Vandamme, John Wiley and Sons, 2009, pp. 197–221.
12 B. Ramprakash and A. Incharoensakdi, *Bioresour. Technol.*, 2020, **318**, 124057.
13 S. Cestellos-Blanco, H. Zhang, J. M. Kim, Y. X. Shen and P. D. Yang, *Nat. Catal.*, 2020, **3**, 245–255.
14 Y. C. Ding, J. R. Bertram, C. Eckert, R. R. Bommareddy, R. Patel, A. Conradie, S. Bryan and P. Nagpal, *J. Am. Chem. Soc.*, 2019, **141**, 10272–10282.
15 Y. Honda, H. Hagiwara, S. Ida and T. Ishihara, *Angew. Chem., Int. Ed.*, 2016, **55**, 8045–8048.
16 S. F. Rowe, G. N. L. Le Gall, E. V. Ainsworth, J. A. Davies, C. W. Lockwood, L. Shi, A. Elliston, I. N. Roberts, K. W. Waldron and D. Richardson, *ACS Catal.*, 2017, **7**, 7558–7566.
17 Y. Honda, M. Watanabe, H. Hagiwara, S. Ida and T. Ishihara, *Appl. Catal., B*, 2017, **210**, 400–406.
18 B. Wang, K. M. Xiao, Z. F. Jiang, J. F. Wang, J. C. Yu and P. K. Wong, *Energy Environ. Sci.*, 2019, **12**, 2185–2191.
19 W. Wei, P. Q. Sun, Z. Li, K. S. Song, W. Y. Su, B. Wang, Y. Z. Liu and J. Zhao, *Sci. Adv.*, 2018, **4**, eaap9253.
20 J. L. Guo, M. Suastegui, K. K. Sakimoto, V. M. Moody, G. Xiao, D. G. Nocera and N. S. Joshi, *Science*, 2018, **362**, 813–816.
21 L. Su and C. M. Ajo-Franklin, *Curr. Opin. Biotechnol.*, 2019, **57**, 66–72.
22 W. Lubitz, H. Ogata, O. RüDiger and E. Reijerse, *Chem. Rev.*, 2014, **114**, 4081–4148.
23 S. Yanagida, A. Kabumoto, K. Mizumoto, C. Pac and K. Yoshino, *J. Chem. Soc., Chem. Commun.*, 1985, 474–475.
24 W. W. Yong, H. Lu, H. Li, S. Wang and M. T. Zhang, *ACS Appl. Mater. Interfaces*, 2018, **10**, 10828–10834.
25 T. M. Swager, *Acc. Chem. Res.*, 1998, **31**, 201–207.
26 H. Lu, R. Hu, H. Bai, H. Chen, F. Lv, L. Liu, S. Wang and H. Tian, *ACS Appl. Mater. Interfaces*, 2017, **9**, 10355–10359.
27 Y. Xiang, X. Wang, L. Rao, P. Wang, D. Huang, X. Ding, X. Zhang, S. Wang, H. Chen and Y. Zhu, *ACS Energy Lett.*, 2018, **3**, 2544–2549.
28 L. Feng, L. Hui, Y. Qu and C. Lv, *Chem. Commun.*, 2012, **43**, 4633–4635.
29 H. B. Yuan, Y. Zhan, A. E. Rowan, C. F. Xing and P. H. J. Kouwer, *Angew. Chem., Int. Ed.*, 2020, **59**, 2720–2724.
30 P. Gai, W. Yu, H. Zhao, R. Qi, F. Li, L. Liu, F. Lv and S. Wang, *Angew. Chem., Int. Ed.*, 2020, **59**, 7224–7229.
31 X. Zhou, Y. Zeng, Y. Y. Tang, Y. M. Huang, F. T. Lv, L. B. Liu and S. Wang, *Sci. Adv.*, 2020, **6**, eabc5237.
32 R. Chai, C. F. Xing, J. J. Qi, Y. B. Fan, H. B. Yuan, R. M. Niu, Y. Zhan and J. L. Xu, *Adv. Funct. Mater.*, 2016, **26**, 9026–9031.
33 Y. X. Wang, S. L. Li, L. B. Liu, F. T. Lv and S. Wang, *Angew. Chem., Int. Ed.*, 2017, **56**, 5308–5311.
34 J. Y. Lin, B. Liu, M. N. Yu, C. J. Ou, Z. F. Lei, F. Liu, X. H. Wang, L. H. Xie, W. S. Zhu, H. F. Ling, X. W. Zhang, P. N. Stavrinou, J. P. Wang, D. D. C. Bradley and W. Huang, *J. Mater. Chem. C*, 2017, **5**, 6762–6770.
35 Z. Wang, D. Gao, Y. Zhan and C. Xing, *ACS Appl. Bio Mater.*, 2020, **3**, 3423–3429.
36 H. Chen, B. Wang, J. Zhang, C. Nie, F. Lv, L. Liu and S. Wang, *Chem. Commun.*, 2015, **51**, 4036–4039.
37 C. Xing, Q. Xu, H. Tang, L. Liu and S. Wang, *J. Am. Chem. Soc.*, 2009, **131**, 13117–13124.
38 B. T. Bajar, E. S. Wang, S. Zhang, M. Z. Lin and J. Chu, *Sensors*, 2016, **16**, 1488.
39 H. Swaminathan and K. Balasubramanian, *Sens. Actuators, B*, 2018, **264**, 337–343.
40 B. Chica, C. H. Wu, Y. Liu, M. W. W. Adams, T. Q. Lian and R. B. Dyer, *Energy Environ. Sci.*, 2017, **10**, 2245–2255.
41 H. Kotani, T. Ono, K. Ohkubo and S. Fukuzumi, *Phys. Chem. Chem. Phys.*, 2007, **9**, 1487–1492.
42 H. Zhu, N. Song, H. Lv, C. L. Hill and T. Lian, *J. Am. Chem. Soc.*, 2012, **134**, 11701–11708.
43 M. C. Scharber, D. Mühlbacher, M. Koppe, P. Denk, C. Waldauf, A. J. Heeger and C. J. Brabec, *Adv. Mater.*, 2006, **18**, 789–794.
44 P. Maruthamuthu, S. Muthu, K. Gurunathan, M. Ashokkumar and M. V. C. Sastri, *Int. J. Hydrogen Energy*, 1992, **17**, 863–866.
45 Y. Zheng and C. S. Harwood, *Appl. Environ. Microbiol.*, 2019, **85**, e02671.
46 E. K. Heiniger, Y. Oda, S. K. Samanta and C. S. Harwood, *Appl. Environ. Microbiol.*, 2012, **78**, 1023–1032.
47 G. X. Feng, C. Y. Tay, Q. X. Chui, R. R. Liu, N. Tomczak, J. Liu, B. Z. Tang, D. Leong and B. Liu, *Biomaterials*, 2014, **35**, 8669–8677.
48 L. H. Feng, L. B. Liu, F. T. Lv, G. C. Bazan and S. Wang, *Adv. Mater.*, 2014, **26**, 3926–3930.
49 N. Kamal, V. Sabaratnam, N. Abdullah, A. S. H. Ho, S. H. Teo, H. B. Lee and A. V. Leeuw, *J. Microbiol.*, 2009, **95**, 179–188.
50 D. Muzziotti, A. Adessi, C. Faraloni, G. Torzillo and R. D. Philippis, *Microbiol. Res.*, 2017, **197**, 49–55.